Advances in Nano Research, *Vol. 11, No. 3 (2021) 313-326*
https://doi.org/10.12989/anr.2021.11.3.313

Analysis of leaking ratio of sealing device for the intake port of EMC closed integral structure turbine disk through soft computing

Yan Cao*[1], Yousef Zandi[2], Abouzar Rahimi[2], Qingming Fan[1], Yu Bai[1], Junde Guo[1], Leijie Fu[1], Mohamed Amine Khadimallah[3,4], Mohammed Jameel[5] and Hamid Assilzadeh**[6]

[1]*School of Mechatronic Engineering, Xi'an Technological University, Xi'an, 710021 China*
[2]*Department of Civil Engineering,Tabriz Branch, Islamic Azad University, Tabriz, Iran*
[3]*Prince Sattam Bin Abdulaziz University, College of Engineering, Civil Engineering Department, Al-Kharj, 16273, Saudi Arabia*
[4]*Laboratory of Systems and Applied Mechanics, Polytechnic School of Tunisia, University of Carthage, Tunis, Tunisia*
[5]*Department of Civil Engineering, College of Engineering, King Khalid University, Abha, Saudi Arabia*
[6]*Institute of Research and Development, Duy Tan University, Da Nang 550000, Vietnam*

(*Received September 10, 2020, Revised June 30, 2021, Accepted July 26, 2021*)

Abstract. The rotor disk produces an azimuthal velocity component in the space between the rotor and stator of a turbine disk, also known as the rim seal cavity. As part of an empirically study, the rim seal cavity is subjected to a test aimed to count the number of unstable structures and evaluate their rotational speed. An Electronic Control Unit (ECU) has a leak test aperture that is sealed by a sealing device that is selectively disposed in the leak test aperture. Designing pump and compressor machines and units requires the development of dependable seal assemblies that maintain tightness over a long period of time and in a wide variety of pressures and temperature. In the field of electrochemical machining (ECM), heat-resistant and high-strength materials may be machined into complicated forms using this well-known technology. ECM presents some issues as the electrochemical copying of grooves, insulating groove features, slots and mini-holes can cause water leakage due to the poor sealing device of the closed integral structure turbine disk. Sealing devices of rotor turbine disks are heavy components with low-cycle fatigue analysis to their life curves. However, there is rare analysis to detect their defects in various rotor regions (temperature, considering stress, mission profile). This study by use of hydro-thermal loading has attempted to focus on the mechanical seals rings and basic productive and operating requirements. Taking the damage and wear, the clearance has been altered that cause a raising in leakage. Generally, the leakage grows more rapidly than linearly with the after-damage clearance. Also, damage and wear were related to the labyrinth seal itself, resulting that the bending curvature and the percentage of bent tooth length were also relevant in defining the leakage in the case of bending damage.
Keywords: ECM; hydro-thermal loading; sealing device; soft computing; turbine disk

1. Introduction

1.1 Sealing device

Assuming the engine as the heart of the automobile, ECUs are its brain. When different components of an automobile (engine, windows, airbags, etc.) react, electronic control units are responsible for controlling how they react (overheating, button pressed by a passenger, crash, etc.) (Shariati 2020, Shariati *et al*. 2020c, g, Li *et al*. 2021). Selectively positioned inside the leak test aperture of an ECU is a sealing device for sealing the leak test aperture, which has an inner surface (Shah *et al*. 2016b, 2020a, h, Duan *et al*. 2021). An opening sealing device is composed of a first part and a second portion that is linked to the first section (Hosseinpour *et al*. 2018, Naghipour *et al*. 2020b, Shariati *et al*. 2020b, Wang *et al*. 2021). A press-fit sealing device is fitted into the leak aperture so that the first portion of the sealing device is in contact with the inner surface, securing the sealing device's position, and the second portion is in contact with the inner surface, preventing moisture and debris from passing through the leak test (Khorramian *et al*. 2016, Khorami *et al*. 2017b, Afshar *et al*. 2020, Ni *et al*. 2020). In terms of size, the second diameter is bigger than its predecessor. Accordingly, the second diameter of the second component exerts a pressure on the inner surface of the leak test aperture while making a sea (Shahabi *et al*. 2016a, Khorami *et al*. 2017a, Trung *et al*. 2019b, Hu *et al*. 2020). When it comes to gas turbine rotor disk sealing devices, they are heavy components and are generally designed using a safe-life method, where the low-cycle fatigue analysis is carried out based on design life curves with appropriate probabilistic margins (Shariati 2013, Arabnejad Khanouki *et al*. 2016, Chen *et al*. 2019b, Suhatril *et al*. 2019, Deng *et al*. 2021). As a result of the weight of the rotor, there is a risk of unnoticed flaws (considering stress, temperature, mission profile) (Sinaei *et al*. 2012, Guarneros-Meza 2016, Khorramian *et al*. 2017, Milovancevic *et al*. 2019).

*Corresponding author, Ph.D.,
E-mail: jantonyz163@aol.com
**Co-corresponding author, Ph.D.,
E-mail: hamidassilzadeh@duytan.edu.vn

ISSN: 2287-237X (Print), 2287-2388 (Online)

There is a direct alignment between performance and engine clearances. For example, it found that advances in fluid film sealing that resulted from a planned study program might save roughly 37 million barrels of oil (1.554 billion = 1554 million gallons) each year, or 0.3% of the U.S.'s energy usage (Shah *et al*. 2016a, Nosrati *et al*. 2018, Toghroli *et al*. 2018, Jiang *et al*. 2021a). Researches could lead to an annual energy saving, on a national basis, equivalent to about 37 million barrels (1.554 billion = 1554 million U.S. gallons) of oil or 0.3% of total U.S. energy consumption. Regarding the engine bleed, Moore (Moore 1975) cited that 1% decrement in engine bleed provides 0.4% decrement in specific fuel consumption (SFC) that translates into roughly 0.033 to 0.055 billion gallons of U.S airlines fuel savings and nearly 0.28 billion gallons in the globe per year. With respect to HPT tip clearance, Lattime and Steinetz (Lattime *et al*. 2002) report an improvement of 0.0254 mm (0.001 inch) results in a reduction of SFC by 0.1% and EGT (exhaust gas temperature) by 1°C, which results in an annual savings of 0.02billion gallons for United States Airlines (US Air). Munson et al. (Munson *et al*. 2002) anticipate fuel savings of approximately 0.5 billion gallons with improved sealing.

The most cost-effective way to improve turbomachinery performance is to control interface clearances (Arabnejad Khanouki *et al*. 2010, Arabnejad Khanouki *et al*. 2011, Shariati *et al*. 2012a). Turbine seals regulate turbo-machinery leaks, coolant flows, as well as overall system rotor dynamic stability like lubricants, sealing interfaces and coatings are often sacrificed for the beneficial of a component (Sinaei *et al*. 2011, Goudarzi *et al*. 2016, Davoodnabi *et al*. 2019, Xie *et al*. 2019, Zhang *et al*. 2019). All of these factors, together with variations in temperature and aerodynamic loads and foreign object damage (FOD), make them vulnerable to erosion, abrasion, oxidation, incursive rubs as well as foreign object damage (FOD) (Shariati *et al*. 2012e, 2014b, 2017, Wei *et al*. 2018). Turbomachinery sealing demands require a range of seal styles and materials. In order to preserve the interface clearance, these seals must be correctly designed and manufactured (Mohammadhassani *et al*. 2014a, Tahmasbi *et al*. 2016, Li *et al*. 2019, Luo *et al*. 2019, Feng *et al*. 2020). If necessary, neighboring surfaces can be machined, while in many other situations coatings are used to optimize performance (Hamidian *et al*. 2011, Shariati *et al*. 2018, 2019b, Rezaeian *et al*. 2020, Ye *et al*. 2020). Numerous seals are constructed from superstructure or substrate composite materials that may be repaired in situ or by stripping, recoating, and reinstalling the seal until the substrate life is surpassed (or until the seal is no longer effective) (ChuppÃ *et al*. 2007, Shariati *et al*. 2010, 2016c, Shahabi *et al*. 2016b, Heydari *et al*. 2018). Fig. 1 shows ECM internal flow channel experiment device, also Fig. 2 shows the device of ECM internal flow channel.

The non-moving stator wall and the spinning blade disk must be separated by a gap below the hub end wall surface (Daie *et al*. 2011, Zhou *et al*. 2011, Mohammadhassani *et al*. 2014c, Nasrollahi *et al*. 2018, Paknahad *et al*. 2018). A boundary layer contact with the rotor disk imparts momentum to the fluid within the rim seal chamber, causing

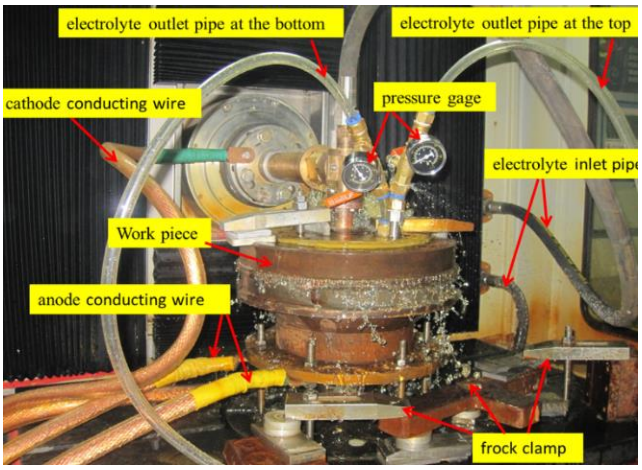

Fig. 1 ECM internal flow channel experiment device

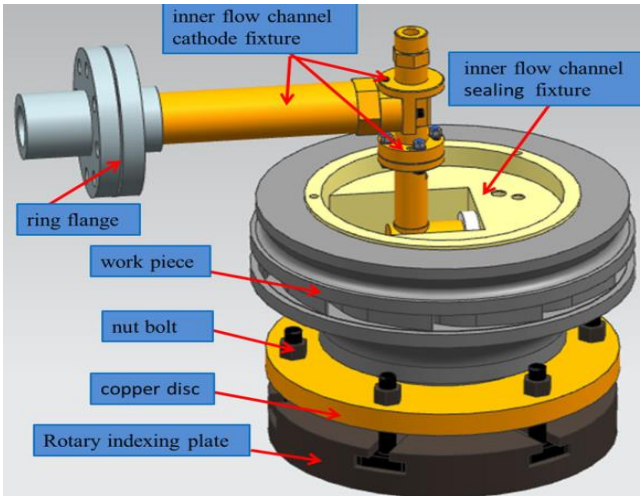

Fig. 2 Device of ECM internal flow channel

the air to swirl (Shariati 2008, 2019a Zandi *et al*. 2018, Naghipour *et al*. 2020a). Turbomachinery design is heavily influenced by turbine flow interactions near rim seals, which impact the aerothermal function of stage (Chen *et al*. 2019a, Sajedi *et al*. 2019, Razavian *et al*. 2020, Jiang *et al*. 2021b, Mehrabi *et al*. 2021). To prevent the hot main annulus gas from being ingested into the turbine disc chamber, extra cooling air is often necessary (Shariati *et al*. 2011a, 2015, 2018, Katebi *et al*. 2019). As the cooling air and primary turbine gas flow interact, the rim seal design may have an effect on aerodynamic losses (Shariati *et al*. 2012c, d, 2014a, 2016, Wang *et al*. 2018). An array of high- and low-pressure cells travels within the rim seal cavity as the swirl system develops (Shariati *et al*. 2011b, 2012b, 2013). In a theoretical and practical investigation of a two-stage turbine, Cao et al. found the cells (Lucas 1990). There is a conclusion from the data that eight unstable constructions are moving at 90 to 97% of their rotor speed. A blade passing occurrence has no bearing on the structures present. Improved aero-thermal performance of an axial flow turbine requires a thorough understanding of the unstable structures in the rim seal cavity (Mohammadhassani *et al*. 2013, Toghroli *et al*. 2014, 2016, Mansouri *et al*. 2019). A three-part study by Phadke and

Owen (Bayley *et al*. 1970, Owen *et al*. 1980, Phadke 1985) into the seals of gas turbine rotor stator systems identified two distinct processes governing the absorption of fluid from the main gas channel into the wheel interior. Simple seal arrangements between a revolving and stationary disk with an empty outer annulus were tried by the authors. The purge flow rate, rotor speed, seal geometry and annulus flow rate may be changed. In addition, they might cause pressure fluctuations in the annulus as a result of their presence. A flow visualization, concentration readings, and pressure measurements were all part of their examination. At small values of Re_w/Re_θ, it is the needed purge flow ratio to seal the wheel space raised by raising Re_θ.

Re_w = *the Reynolds number of annulus flow*
Re_θ = *the rotational Reynolds number*

At large values of Re_w/Re_θ, the needed purge flow ratio to seal the wheel space was independent of Re_θ and highly based on the pressure variation in the annulus (Sadeghipour Chahnasir *et al*. 2018, Sedghi *et al*. 2018, Katebi *et al*. 2019, Shariati *et al*. 2019e). Externally induced (EI) and Rotationally induced (RI) ingress are the physical processes that regulate these two regimes (Shariati *et al*. 2019c, d, 2020e, 2021a, Partovi *et al*. 2020). An orifice model by Owen (Phadke *et al*. 1983) was used to investigate the reason of EI intrusion and compare the experimental data results and 3-D computational fluid dynamics (CFD). It was also observed that the pressure difference in the primary gas channel showed a substantial association with gas entry, as Phadke and Owen had found. A greater static pressure in the wheel space produced entrance, while a lower one caused egress from the wheel space and out of it into the main air flow route. The vane wakes create the high pressure in the hot gas route, whereas the clean flow through the vane passageways causes the low static pressure in hot gas path. Owen further demonstrated that the form of the circumferential pressure fluctuation was related to the pattern of intake. A fundamental fluid dynamics argument was used to explain RI ingress by Sangan, Lalwani, Owen, and Lock (Phadke *et al*. 1988). As a spinning disk spins in a stationary fluid, a boundary layer forms over the disk and fluid is expelled radially. A radial flow of fluid must be countered by an axial flow of fluid toward the revolving disk. One disk is fixed while the other is spinning in turbomachines. With a revolving fluid core between the two disks, distinct boundary layers arise (Safa *et al*. 2020, Shariati *et al*. 2020d, f, Yazdani *et al*. 2020, Nouri *et al*. 2021). A radially inward pressure gradient balances the centrifugal force on the core fluid. In order to generate the radial pressure gradient, the core fluid must move more slowly at smaller radii than at larger radii. Fluid rotation is slowed near a stationary wall due to no-slip conditions, leaving it with less centrifugal force than that provided by the pressure gradient throughout its radius (Mohammadhassani *et al*. 2014b, Safa *et al*. 2016, Trung *et al*. 2019a, Jahandari *et al*. 2021, Shariati *et al*. 2021). Thus, the radial pressure gradient causes fluid to flow down the wall of the stationary disk due to its radial pressure gradient effect (Qi *et al*. 2019, 2020, Huang *et al*. 2021, Jiao *et al*. 2021, Ma *et al*. 2021, Zhao *et al*. 2021). It is because of this

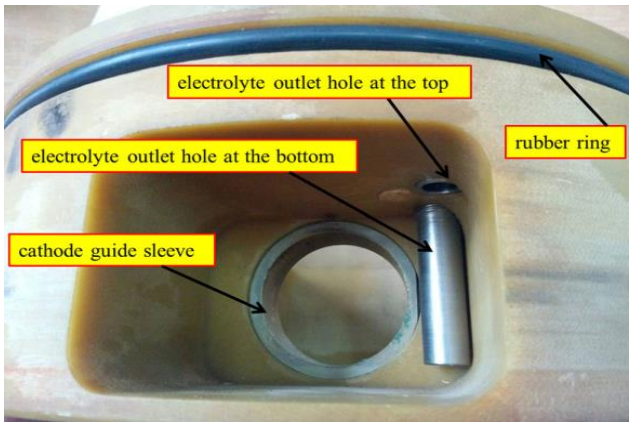

Fig. 3 The device of adjusting electrolyte outlet pressure

Fig. 4 Rings of friction pairs of mechanical seals

flow of fluid that a large amount of air is drawn into the wheel area from the main gas channel. Purge flow can be used to decrease or eliminate the ingress of fluid from the primary gas route. In addition, purge flow balances mass conservation of fluid exiting the wheel space owing to disk pumping and prevents fluid from being swallowed along the stator wall (Shariati *et al*. 2011c, Shah *et al*. 2015, Ziaei-Nia *et al*. 2018). Double-rim seals, which seal the wheel space more effectively with less purge flow, are generally more engine representative than radial or axial seals. Phadke and Owen (Phadke 1985) have shown that flows entering the wheel space of one rim system may traverse vast parts of the wheel space using flow visualization techniques. According to their flow visualization research, when a double rim seal was placed, flow entering the wheel area was limited to the outside region and did not cross the second rim seal. There was a comparison between three distinct types of computational research by Jakoby et al (El-Oun *et al*. 1988). Fig. 3 shows the device of adjusting electrolyte outlet pressure. A 360-degree examination of the rim seal cavity is the test that best depicts the structures within the cavity. They're traveling at 80 percent of the rotor speed because of the rim seal cavity. Fig. shows the rings of friction pairs of mechanical seals.

1.2 ECM machines

Since 1780, electrochemical dissolution has been used

to remove metals, but it has only been exploited to its full potential in the last two decades. Contactless electro-chemical forming process is another name for this technique. Due to the fact that electrical energy is employed to generate a chemical reaction, electrochemical machining was born (ECM). Electrolysis follows Faraday's laws. By placing the two electrodes in a conductive liquid bath and applying DC voltage (5-25V) across them, Michael Faraday discovered that metal could be removed from the anode and deposited on a second electrode. In the past, this idea was widely used. Electroplating is reversed in ECM. As an electrochemical method, ECM is a process of controlled dissolving at the atomic level of electrically conducting work pieces using an electrolyte, which is usually a water-based neutral salt solution. When using ECM, the electrolyte is selected in such a way that the tool is not plated and its form is not altered. Maintaining a little space between the tool and work (0.1 to 0.2mm) results in a similar-looking machined surface. For many industrial applications such as the manufacturing of complicated aero engine components made from difficult-to-cut materials, electrochemical machining (ECM) has become a feasible option. A number of its benefits are no tool wear, independence from material mechanical characteristics, and great efficiency in machining. By degrading materials from work piece by electrochemical dissolution at atomic level, electrochemical machining (ECM) is able to produce complex forms and geometries on a wide range of sophisticated technical materials (Das *et al*. 2020). Machines made with ECM are ideal for machining tough materials since it does not depend on work piece hardness (Schubert *et al*. 2018). With ECM machining, the tool and the work piece aren't exposed to as much heat as with other methods of machining (Sathiyamoorthy *et al*. 2015). Aside from avoiding heat stress and tool wear, ECM may also create complicated forms and shiny surfaces without the need for any extra procedures (Lohrengel *et al*. 2016). Using an electrochemical technique is a way of removing metal. Electrochemical metallization (ECM) is sometimes known as reverse electroplating, in which material is removed instead of being deposited (Todd *et al*. 1994, Valenti 2001). It is typically utilized for mass manufacturing and for dealing with exceptionally hard materials or materials that are difficult to process using traditional techniques, such as titanium and aluminum. Electrically conductive materials are the only materials that can be used with it. When using ECM, the cutting tool is directed along the required route near to the work piece, but without contacting the work piece directly. To the contrary, no sparks are produced in this style of music. As long as no heat or mechanical stress is transmitted to the component, high metal removal rates may be accomplished with ECM. A cathode is advanced into an anode during the ECM process. Electricity is applied to the cutting region by injecting a pressurized electrolyte at a certain temperature. Material liquefaction rate equals the feed rate (Valenti 2001). In between the tool and the work piece, there is a space of 80 to 800 micrometers, depending on the tool. Material from the work piece dissolves when electrons traverse the gap, as the tool creates a shape in the work

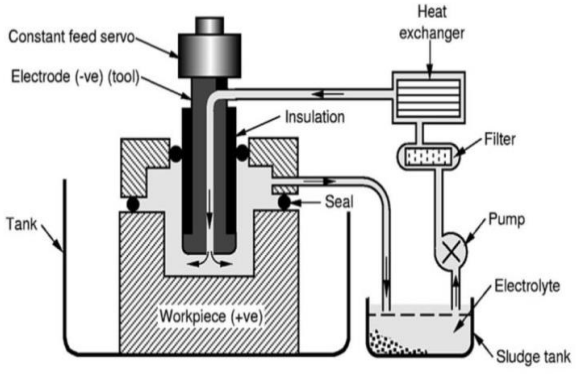

Fig. 5 Principle of ECM, adapted after Anonymous, (2010)

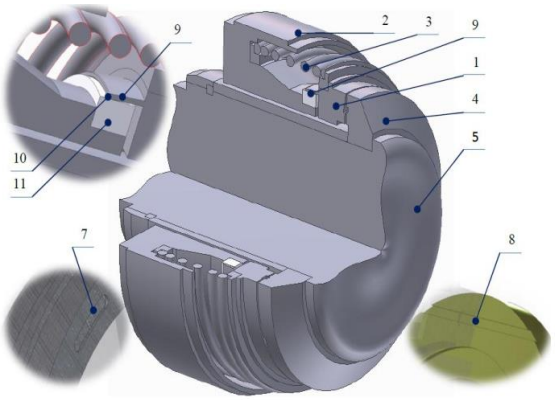

Fig. 6 The seal comprises an axially movable ring

piece. As a result of the procedure, metal hydroxide is removed by the electrolytic fluid. ECM can cut small or odd-shaped angles, showing contours or cavities for exotic and hard metals, such as high nickel, titanium aluminides, cobalt and rhenium alloys. It is possible to manufacture both exterior and interior geometries. To manufacture complex forms such as turbine blades with an excellent surface quality from tough to machine materials, the ECM method is frequently employed. A deburring procedure is also extensively and efficiently utilized with it (Yuan *et al*. 2021). Fig. 5 shows the principle of ECM. The seal includes an axially movable ring with 1, set in housing that 2 is preloaded with spring 3 and the metal supporting ring 4, fixed to shaft 5. At the end of the working surface 6 of the ring 1, there is a set of chambers 7 set across the circumference of ring. On the ring 4, there are some tangential channels 8, with middle portions of which located on the axis at the same distance as the cameras 7. The number of channels 8 is less than the number of cameras 7 so that there is link with the cavity of hardening medium only a part of cameras. This conical whisker has a sealing surface 10 in place of the contact with the sealing surface of the bushing 11 (Fig. 6).

1.3 Purge flow system

1.3.1 Unsteady pressure measurements in the rim seal cavity

These patterns are affected by the structures within the

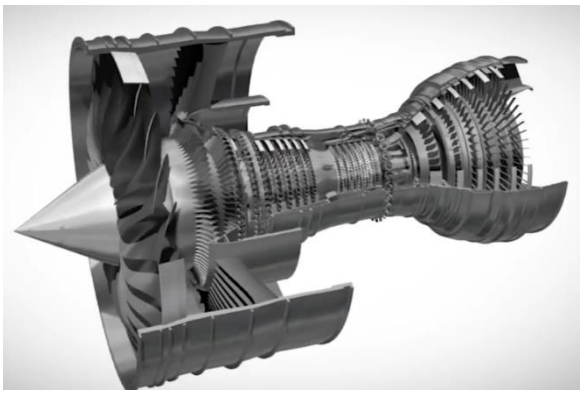

Fig. 7 Simulation plot of Turbine disc

Fig. 8 Production process of turbine disc

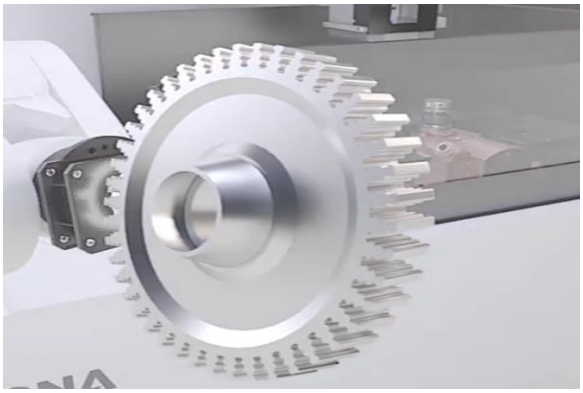

Fig. 9 Simulation production of turbine disc

seal cavity. This pattern of high and low static pressure has been seen in similar buildings in the past. There's a way to calculate the speed and quantity of structures present at any time if at least two fast response probes are kept at a specified distance apart and can record data concurrently. To measure the unstable structures, Endevco's (8507C-1) unsteady transducers are employed. We created a drawing of the rim seal chamber, which has a double radial seal. A double radial seal geometry is used. As seen in Fig. 6, the cavity next to which the transducers are indicated in red is known as the buffer cavity, and it is positioned between the outer and inner seals. There is a serpentine channel below the inner seal that the injected purge flow must follow to reach the rim seal hollow. There are periodic inlets positioned around the inner circumference of the annulus that are used to mix and settle fluids in this flow channel with rim seals. Further details of the rim seal chamber design are provided by Averbach (Ko *et al*. 1992). In the same radial location, the two pressure transducers are spaced 5 mm apart. In order to determine the speed and quantity of structures within the rim seal cavity using our technique, at least two probes that can capture data concurrently are essential. Fig. 7 shows the simulation plot of Turbine disc; Fig. 8 indicates the production process of turbine disc, while Fig. 9 indicates the simulation production of turbine disc.

2. Turbine discs

Significant-speed turbine discs in a cold environment are subjected to high rotating stresses. The disc's resistance to fatigue cracking is the limiting factor for its usable life. Ferritic and austenitic steels have been utilized in the past, but nickel-based alloys are now employed. Due to increased fatigue resistance, adding the alloying elements in nickel can lengthen the lifespan of a disc. Alternatively, powder metallurgy discs, which are high cost, but give a 10 percent increase in strength, can be used to reach higher rotating speeds.

2.1 Blades of a turbine

The importance of choosing the right material for turbine blades may be illustrated by mentioning a few of the factors to consider while designing turbine blades. The red-hot blades must be robust enough to withstand the centrifugal forces created by the high-speed rotation. In order to operate the compressor, a tiny turbine blade weighing just 2 ounces may impose a force of nearly 2 tons at peak speed, and it should endure the tremendous bending stresses produced by the gas. Also, turbine blades should withstand high-frequency variations in gas conditions, as well as corrosion and oxidation. A material that can be properly shaped and machined by existing production processes should still be used to make the blades. A specific blade material and a safe operating life have a maximum permitted turbine entrance temperature and maximum engine power, which derives from the above. The ongoing search for better turbine blade materials and enhanced blade cooling techniques by metallurgists and designers is not unexpected. The turbine blades gradually expand in length over time. "Creep" is a term used to describe this process, and there is a finite usable life limit before failure occurs. When high temperature steel forgings became popular, they were quickly supplanted by cast nickel base alloys with improved creep and fatigue characteristics. There are many crystals on typical turbine blades (equiaxed). By aligning the crystals to create columns along the blade's length, a process of "directional solidification," the blade's service life can be extended. Making the blade out of a single crystal is a step up from this approach. As a result of each of these methods, the blade's usable creep life may be extended. In addition, the working temperature of a single crystal blade can be significantly raised. Reinforced

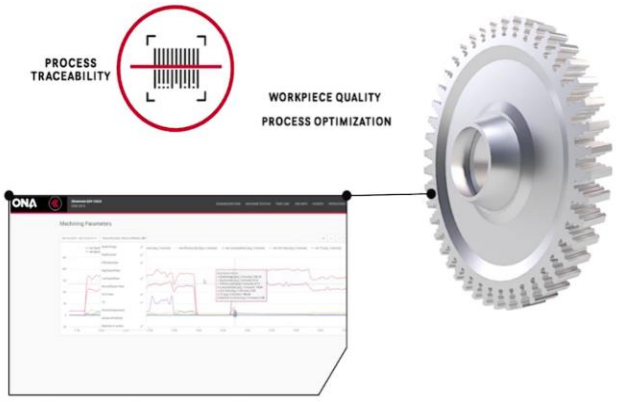

Fig. 10 The function of turbine disc through simulator

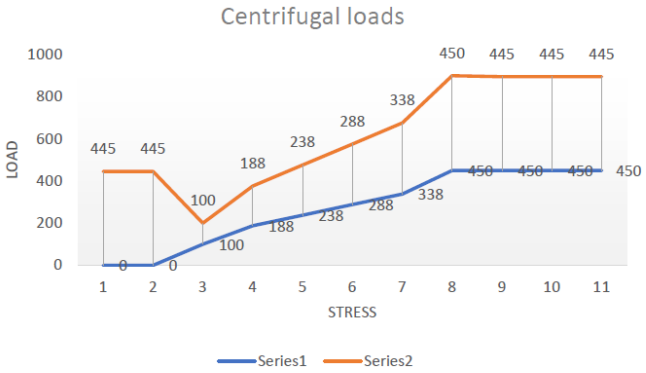

Fig. 11 Assessment of a turbine disc: (a) state of stress due to primary centrifugal loads

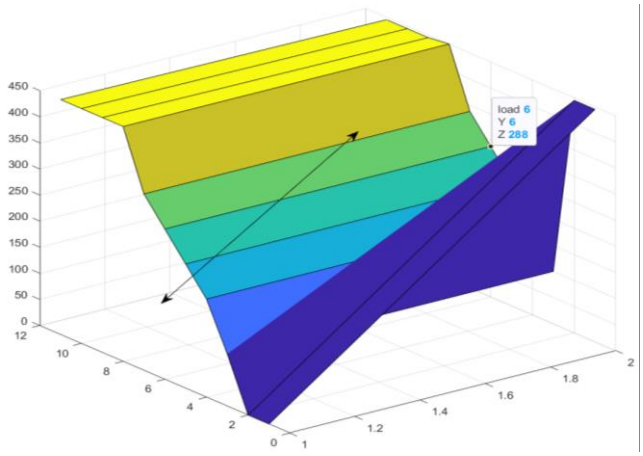

Fig. 12 FE elastic–plastic analyses for the verification of β, global model

ceramics can be used to create a turbine blade that is not made of metal. A tiny high-speed turbine with high turbine entrance temperatures may be their first use. Some of the problems involved in increasing a gas turbine's power and temperature limits may be seen in the following example. Gas turbine OEM (original equipment manufacturers) vendors are determined by the quality of their financial services. GE is the uncontested leader in financial services, as seen by the size of its fleets, especially in newly developing nations. It has been proven that other OEMs have created profitable joint ventures with international power firms and banks (Tang *et al*. 2017). It is possible that the inadequate sealing mechanism of the closed integrated structure turbine disk causes leakage of water while electrochemically duplicating slots, micro holes, grooves, and insulating groove characteristics in electrochemical machining. Determining what kind of seal is needed for a long period in various temperatures and pressures is crucial to the design process of ECM closed integrated structure turbine disks and units. Fig. 10 indicates the function of turbine disc through simulator. Fig. 11 is the assessment of a turbine disc: (a) state of stress due to primary centrifugal loads and Fig. 12 shows the FE elastic–plastic analyses for the verification of β, global model.

3. Sealing device for the ECM intake port

In gas turbine engines and other friction units, the performance of bearings depends heavily on the quantity of heat transmitted into the surrounding oil cavity and the degree of leakage. Part of the heat is absorbed by the seal with working gas and the support's wall. As a result, the quantity of heat generated by various sources might reach up to 80%. In many cases, the reliability of sealing systems determines contemporary aircraft engines' dependability and durability. The raised rotor speed, temperature, pressure, and velocities in the gas passage complicate the seal's operating conditions owing to increased thermal stress (Martin 1908). Seal research may be approached from two different angles. Seals are regarded a frictional pair whose functioning capability must be assured in the initial approach. As part of the engine system, the seal is considered in the second method. The engine oil system seal's functioning, as well as the effect of processes occurring in the seal during the oil system's operation, should be closely examined (Egli 1935). Hart (Kearton *et al*. 1952) and Kingsporn (Schramm *et al*. 2002) demonstrate the tight relationship between the heat flow and the supporting element, as well as the elements that feed oil to the friction bearing nodes. As a result, the oil in the engine supporting element should be heated between 40 and 70 degrees Celsius. With current engine temperatures, it's nearly impossible to meet this criterion. The additional heat flow might also cause the oil mixture in the bearing cavity to catch fire due to the increased heat flow. There are experimental studies of ignition conditions (Wittig *et al*. 1983). The oil from friction units is extremely difficult to remove. In the works (Bill *et al*. 1977, Demko *et al*. 1990), problems related to the design of breathers are discussed. Afterburner turbofan engines and turboprop engines were examined for oil consumption in this study. From the analysis of the Fig. 14, the graphs illustrate the relationship between oil consumption and thrust or power for various. The engine's technical description is used to determine the values. There is a 15-times increase in compressor pressure ratio and a two-time increase in gas temperature prior the turbine from 1000 K to 2000 K (Stewart *et al*. 1978). It is concluded that the amount of oil consumption is dependent on the engine thrust (power). It is on 40 - 50% more that largely is dependent on the reduction gear usage for

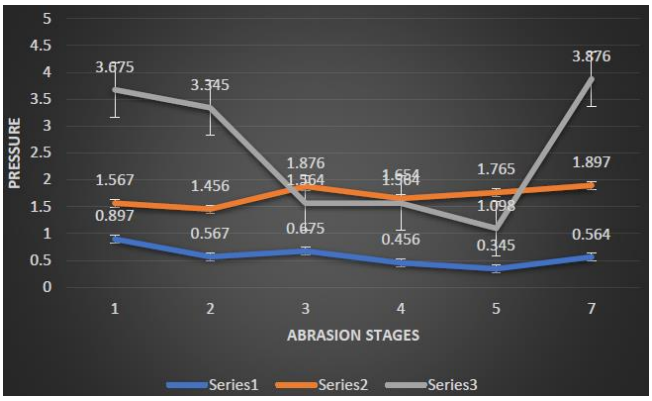

Fig. 13 The stages of abrasion:1 – cold burnishing; 2 – stable abrasion; 3 – destructive abrasion

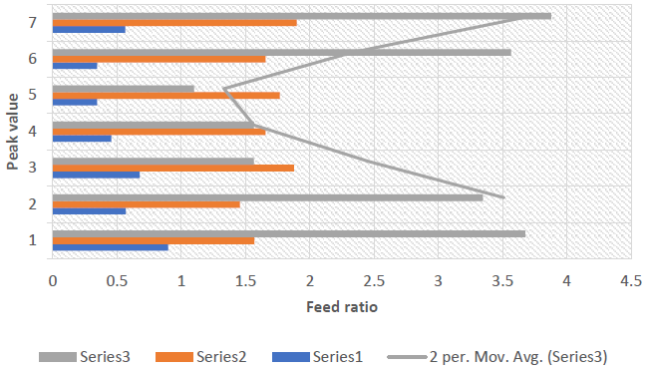

Fig. 14 Variation of side gap with cathode feed rate in the different feed modes

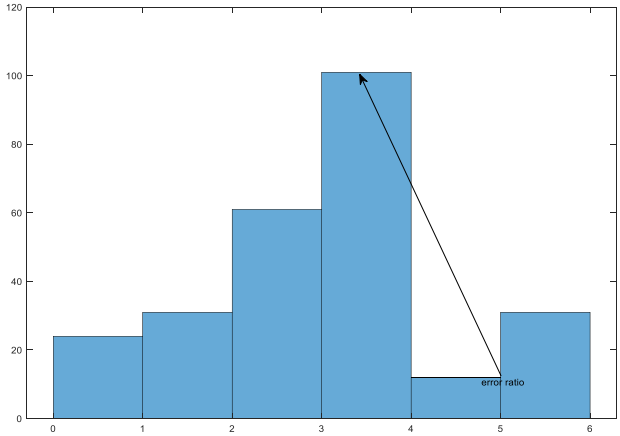

Fig. 15 The error percentage of ECM tool retraction followed by the repositioning

turboprop engines. Heat flow through the engine supports is another element that affects oil consumption and may be influenced. On a plane engine (Figs. 5 and 6), it demonstrates the experimental changes in oil consumption across three different supports. The front support consumes the least amount of energy, while the middle and back support consume the most. Consumption values differ by more than 3 times because of the high temperature of ambient air (gas), and to the volume of oil cavity. Fig. 13 indicates the stages of abrasion:1 – cold burnishing; 2 – stable abrasion; 3 – destructive abrasion. Fig. 14 is the variation of side gap with cathode feed rate in the different feed modes. Fig. 16. Graph illustrating the evolution of the current peak value of the pulses.

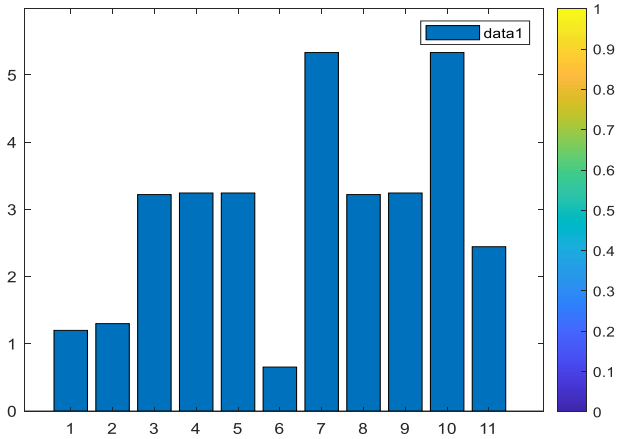

Fig. 16 Graph illustrating the evolution of the current peak value of the pulses

3.1 Numerical analysis of leak rate prediction model

Fig. 15 shows the error percentage of ECM tool retraction followed by the repositioning and Fig. 16 shows the graph illustrating the evolution of the current peak value of the pulses. It has been shown in Ref (Greenwood *et al.* 1970) that contact between a rigid flat surface and a rough, fractal surface may be modelled as the contact between two surfaces. According to research (Heinze 1949, Jana *et al.* 2017), seal surfaces have self-affine features that may be approximated using the three-dimensional Ausloos–Berman function. The following model is applied to compute the static sealing surface by high precision grinding:

$$z(x,y) = L\left(\frac{G}{L}\right)^{D-2}\left(\frac{In\,\gamma}{M}\right)^{1/2}\sum_{m=1}^{M}\sum_{n=n_1}^{n_{max}}\gamma^{(D-3)n} \quad (1)$$

$$*\left\{\cos\emptyset_i - cos\left[\frac{2\pi\gamma^n(x^2+y^2)^{\frac{1}{2}}}{L}cos\left(arctan\left(\frac{y}{x}\right)-\frac{\pi m}{M}\right)+\emptyset_a\right]\right\} \quad (2)$$

z = *the height*

(x,y) = *the coordinates of surface*

The surface roughness is defined by the frequency spectrum γ^n, in which γ satisfies $\gamma > 1$; n indicating the frequency index of asperities.

M = used to construct the surface and denotes the number of superposed

L = sample length

$\emptyset_a$ *= a random number in the range of 0 and 2p*

D (which lies in the domain of 2 < D < 3) = fractal dimension

G = the roughness constant (D and G are independent of γ*)*

$$S_G = \frac{4}{3}\sqrt{\pi}E(g_1(D)C^*)^{\frac{1}{2}}g_2(D)\psi^{(D-\frac{2)^2}{4}}A_r^{*\frac{D}{2}} \quad (3)$$

$$\left[\left(\frac{2-D}{D}\psi^{\frac{D-2}{2}}A_{\mathrm{r}}^{*}\right)^{\frac{3-2D}{2}}-a_{\mathrm{c}}^{*\frac{3-2D}{2}}\right] \quad (4)$$

$$\left[Ek_{\mathrm{y}}\varphi g_3(D)\psi^{(D-\frac{2)^2}{4}}A_{\mathrm{r}}^{*\frac{D}{2}}a_{\mathrm{pe}}^{*\frac{2-D}{2}}+\frac{2}{3}E\varphi g_3(D)\psi^{(D-\frac{2)^2}{4}}A_{\mathrm{r}}^{*\frac{D}{2}}\right. \quad (5)$$

$$\left[2+\ln\left(\frac{\sqrt{\pi}(g_1(D)C^{*})^{\frac{1}{2}}}{3\varphi}\right)\right]\left(a_{\mathrm{c}}^{*\frac{2-D}{2}}-a_{\mathrm{pe}}^{*\frac{2-D}{2}}\right) \quad (6)$$

$$\left[\frac{1-D}{3}E\varphi g_3(D)\psi^{(D-\frac{2)^2}{4}}A_{\mathrm{r}}^{*\frac{D}{2}}\right. \quad (7)$$

$$\left.a_{\mathrm{c}}^{*\frac{2-D}{2}}\ln(a_{\mathrm{c}}^{*})-a_{\mathrm{pe}}^{*\frac{2-D}{2}}\ln(a_{\mathrm{pe}}^{*})-\frac{2}{2-D}\left(a_{\mathrm{c}}^{*\frac{2-D}{2}}-a_{\mathrm{pe}}^{*\frac{2-D}{2}}\right)\right] \quad (8)$$

Considering the assumption (Zhang *et al*. 2018) the cross-sectional profile of the asperity and pore are as follows:

$$z(x)=G^{D-2}(\ln\gamma)^{\frac{1}{2}}l^{(3-D)}\left[1-cos\left(\frac{2\pi x}{l}\right)\right](0<x<l) \quad (9)$$

$$z_v(x)=G^{D-2}(\ln\gamma)^{1/2}l_v^{(3-D)}\left[\cos\left(\frac{2\pi x}{l_v}\right)\right](0<x<l_v) \quad (10)$$

$$n_l(l)=(D-1)l_{max}^{D-1}l^{-D} \quad (11)$$

$$n_{l,v}=(D-1)\left[\frac{4(3-D)A_t}{\pi(D-1)}-l_{max,v}^2\right]^{\frac{D-1}{2}}l_p^{-D}, \quad (12)$$

4 . Thermal-hydraulic analysis

Energy system operation planning relies on hydro thermal scheduling. Scheduling of hydroelectric units and thermal units are the primary issues. The water outflow from one plant can, however, constitute a major percentage of the intake to one or more downstream plants when many hydro plants are located on the same river. In both electric and hydraulic couplings, a non-linear, multi-dimensional issue is created. Optimizing the generation in a hydro thermal system entails splitting up the generation between hydel and thermal units, in order to minimize the overall operating cost of thermal plants while meeting all of its different restrictions. Normally, in short-term scheduling, it's expected that a medium-term planning process that takes into consideration long-term river inflow modeling and load forecasts has established the target dam levels at the conclusion of the scheduling period. Hydro power generation is subsequently allocated to various time intervals by the short-term scheduler in order to reduce thermal production costs while fulfilling various unit and reservoir restrictions. Cascade nature of hydraulic network, varying hourly reservoir inflows, thermal plants, the time coupling effect of the hydro sub problem where the varying system load demand and physical limitations of reservoir storage are limitations. Artificial neural networks, expert systems, network flow and linear programming, dynamic programming, nonlinear programming and mathematical decomposition are some important solution methods. l-g iteration, gradient technique, and dynamic programming methods are the three most commonly utilized solutions for hydrothermal scheduling problems. However, each has its own disadvantages. Solving coordination equations in the l-g iteration approach leads to plant generations that are beyond plant capacity and even negative plant generations in some cases. The value of g would vary if plant capacity, volume, and hourly discharge restrictions were added. This would need the scheduling mechanism to modify g such that the restricted variable does not exceed its limit. In big systems, the gradient technique is proven to be inefficient (El-Hawary *et al*. 1979). Each reservoir's initial viable schedule has to be specified when using the dynamic programming technique with successive approximation method (Jin-Shyr *et al*. 1989). As a result, one reservoir is scheduled while the others are not. This is repeated until given iterations, or the cost difference between two iterations is within provided tolerance. Only one reservoir may be sent at a time; therefore, this approach is not flexible enough to handle coupling limitations.

$$\begin{aligned}&V_h(i,t)^{min}\le V_h(i,t)\le V_h(i,t)^{max};t\in T\\&Q_h(i,t)^{min}\le Q_h(i,t)\le Q_h(i,t)^{max};t\in T\end{aligned} \quad (13)$$

$$\begin{aligned}&V_h(i,t)|_{t=0}=V_{h,i}{}^{\text{beggin}};i\in R_h\\&V_h(i,t)|_{t=T}=V_{h,i}{}^{\text{end}};i\in R_h\end{aligned} \quad (14)$$

$$V_h(i,t)=V_h(i,t-1)+I_h(i,t)-Q_h(i,t)-S_h(i,t)+\sum_{m=1}^{Ru}\left[Q_h\big(m,t-\tau(i,m)\big)+S_h\big(m,t-\tau(i,m)\big)\right] \quad (15)$$

$$\sum_{i=1}^{Rs}P_s(i,t)+\sum_{i=1}^{Rh}P_h(i,t)\ge R_{req,t} \quad (16)$$

$$P_h(i,t)=f\big(Q_h(i,t),V_h(i,t)\big) \quad (17)$$

The model could also be written in terms of reservoir volume instead of reservoir net head

$$\begin{aligned}&P_h(i,t)=C_{1,i}V_h(i,t)^2+C_{2,i}Q_h(i,t)^2\\&C_{3,i}(V_h(i,t)^{*}Q_h(i,t))+\\&C_{4,i}V_h(i,t)+C_{5,i}Q_h(i,t)+C_{6,i};i\in Rh\\&Q_j{}^t max=\text{Min}\left\{Q_{jmax},\left(V_j^{t-1}+Q_{j-1}^{t-1}+I_j{}^t-V_{jmin}\right),\right.\\&\left.\left(-V_{j+1}{}^{t-1}-I_{j+1}{}^t+Q_{j+1max}+V_{j+1max}\right)\right\}\ (11)\\&Q_j{}^t min=\text{Max}\left\{Q_{jmin},\left(V_j{}^{t-1}+Q_{j-1}{}^{t-\tau}+I_j{}^t-V_{jmax}\right)\right.\end{aligned} \quad (18)$$

$$=\left|\begin{array}{c}\sum_{i\in Rh}\psi\big(Vh,i(\text{ end})\big)\\\sum_{i\in Rh}C_{2,i}Qh,\text{ex}(i,t)^2+C_{5,i}Qh,\text{ex}(i,t)+\\C_{3,i}(Vh(i,t))^{*}Qh,\text{ex}(i,t)\big)+C_{6,i}\end{array}\right| \quad (19)$$

*IC

5. Conclusions

The damage and wear of the labyrinth seal had a considerable impact on the leakage and temperature fields, as well as the flow pattern. As a result of damage and wear, the clearance has been changed, causing an increase in leakage. Generally, the leakage grows more rapidly than linearly with the after-damage clearance. Additionally, damage and wear patterns were discovered to be relevant in addition to the labyrinth seal itself. It was observed that the bending curvature and the percentage of tooth length that is bent were also relevant in determining the leakage in the case of bending damage. Using adiabatic walls, the current work examined the temperature field in the rim-cavity to isolate the influence of labyrinth seal rub grooves on ingress heating. ECM and related processes are described in terms of their operating concept and application. The ECM method may be used to fabricate complex forms with high material removal rates and good surface quality. It's a potential approach for micromachining crucial components that doesn't affect the material's thermal and mechanical characteristics. Process stability is affected by the electrolyte flow field, especially for closed integer impellers. Three-dimensional gap flow simulation model and theoretical model were developed to increase the stability and machining quality of the machining process. Following simulation findings, cathode and frock clamp designs were developed. A closed integer impeller may be machined more efficiently with a model B cathode structure, as shown by the simulation results. During the ECM verification trials, the cathode and internal flow channel ECM fixture were evaluated for their logical design and effectiveness. When employing the cathode of model B, a fixture, and the appropriate machining settings, the findings demonstrate that steady milling is possible. A flow field simulation aided cathode design is helpful and inexpensive for ECM process closed impeller internal flow channel, which is an effective way to minimize ECM costs and increase machining efficiency for the closed integer impeller. To manufacture irregular vortex paths with great efficiency and precision by combining the technologies of ECM, it has a significant practical application value. ECM is used to prepare for EDM precision machining by machining interior channels with consistent allowances.

Acknowledgment

This paper is supported by Xi'an Science and Technology Project (Grant: 2020KJRC0032), Yulin Science and Technology Project (Grant: 2019-122), Shaanxi Key Research and Development Plan (Grant: 2020GY-147), Project of Joint Postgraduate Training Base of Xi'an Technological University, and Research Project of Graduate Education and Teaching Reform of Xi'an Technological University in 2017.

References

Afshar, A., Jahandari, S., Rasekh, H., Shariati, M., Afshar, A. and Shokrgozar, A. (2020), "Corrosion resistance evaluation of rebars with various primers and coatings in concrete modified with different additives." *Constr. Build. Mater.*, **262**, 120034. https://doi.org/10.1016/j.conbuildmat.2020.120034.

Arabnejad Khanouki, M.M., Ramli Sulong, N.H. and Shariati, M. (2010), "Investigation of seismic behaviour of composite structures with concrete filled square steel tubular (CFSST) column by push-over and time-history analyses", *Proceedings of the 4th International Conference on Steel & Composite Structures*. http://doi.org/10.3850/978-981-08-6218-3_CC-Fr003.

Arabnejad Khanouki, M.M., Ramli Sulong, N.H. and Shariati, M. (2011), "Behavior of through beam connections composed of CFSST columns and steel beams by finite element studying", *Adv. Mater. Res.*, **168**, 2329-2333. http://doi.org/10.4028/www.scientific.net/AMR.168-170.2329.

Arabnejad Khanouki, M.M., Ramli Sulong, N.H., Shariati, M. and Tahir, M.M. (2016), "Investigation of through beam connection to concrete filled circular steel tube (CFCST) column", *J. Constr. Steel Res.*, **121**, 144-162. https://doi.org/10.1016/j.jcsr.2016.01.002.

Bayley, F.J. and Owen, J. (1970), "The fluid dynamics of a shrouded disk system with a radial outflow of coolant", *J. Eng. Power.*, **92**(3), 335-341. https://doi.org/10.1115/1.3445358.

Bill, R.C. and Shiembob, L.T. (1977), "Friction and wear of sintered fibermetal abradable seal materials" *J. Lubrication Tech.*, **99**(4), 421-427. https://doi.org/10.1115/1.3453236.

Chen, C., Shi, L., Shariati, M., Toghroli, A., Mohamad, E.T., Bui, D.T. and Khorami, M. (2019a), "Behavior of steel storage pallet racking connection-A review", *Steel Compos. Struct.*, **30**(5), 457-469. https://doi.org/10.12989/scs.2019.30.5.457.

Chen, K., Rui, S.Y., Wang, F., Dong, J.X. and Yao, Z.H. (2019b), "Microstructure and homogenization process of as-cast GH4169D alloy for novel turbine disk", *Int. J. Miner. Metall. Mater.*, **26**(7), 889-900. https://doi.org/10.1007/s12613-019-1802-0.

ChuppÃ, R.E., Hendricks, R.C., Lattime, S.B., Steinetz, B.M. and Aksit, M.F. (2007), "Turbomachinery clearance control", *Turbine Aerodynam. Heat Transf. Mater. Mech.*, **61.** https://doi.org/10.2514/4.102660.

Daie, M., Jalali, A., Suhatril, M., Shariati, M., Arabnejad Khanouki, M. M., Shariati, A. and Kazemi-Arbat, P. (2011), "A new finite element investigation on pre-bent steel strips as damper for vibration control", *Int. J. Phys. Sci.*, **6**(36), 8044-8050. https://doi.org/10.5897/ijps11.1585.

Das, P.P. and Chakraborty, S. (2020), *Parametric Optimization of Electrochemical Machining Process Using Taguchi Method and Super Ranking Concept While Machining on Inconel 825* in *Advanced Engineering Optimization Through Intelligent Techniques*, Springer, Singapore.

Davoodnabi, S.M., Mirhosseini, S.M. and Shariati, M. (2019), "Behavior of steel-concrete composite beam using angle shear connectors at fire condition", *Steel Compos. Struct.*, **30**(2), 141-147. https://doi.org/10.12989/scs.2019.30.2.141.

Demko, J., Morrison, G. and Rhode, D. (1990), "Effect of shaft rotation on the incompressible flow in a labyrinth seal", *J. Propulsion Power*, **6**(2), 171-176. https://doi.org/10.2514/3.23240.

Deng, R., Li, M. and Linghu, S. (2021), "Sensitivity analysis of steam injection parameters of steam injection thermal recovery technology", *Fresenius Environ. Bull.*, **30**(5), 5385-5394.

Duan, X., Deng, B., Liu, Y., Li, Y. and Liu, J. (2021), "Experimental study the impacts of the key operating and design parameters on the cycle-to-cycle variations of the natural gas SI engine", *Fuel*, **290**, 119976. https://doi.org/10.1016/j.fuel.2020.119976.

Egli, A. (1935), "The leakage of steam through labyrinth seals",

Trans. *Asme*, **57**(3), 115-122.
El-Hawary, M.E. and Christensen, G.S. (1979), *Optimal Economic Operation of Electric Power Systems*, New York: Academic Press.
El-Oun, Z., Neller, P. and Turner, A. (1988), "Sealing of a shrouded rotor–stator system with preswirl coolant", *J. Turbomach*., **110**(2), 218-225. https://doi.org/10.1115/1.3262184.
Feng, P., Chang, H., Liu, X., Ye, S., Shu, X. and Ran, Q. (2020), "The significance of dispersion of nano-SiO_2 on early age hydration of cement pastes", *Mater*. *Des*., **186**, 108320. https://doi.org/10.1016/j.matdes.2019.108320.
Goudarzi, A., Ghassemieh, M., Fanaie, N., Laefer, D.F. and Baei, M. (2016), "Axial load effects on flush end-plate moment connections", *Proceedings of the Institution of Civil Engineers-Structures and Buildings*, **170**(3), 199-210. https://doi.org/10.1680/jstbu.15.00042.
Greenwood, J.A. and Tripp, J. (1970), "The contact of two nominally flat rough surfaces", *Proceedings of the Institution of Mechanical Engineers*, **185**(1), 625-633. https://doi.org/10.1243/PIME_PROC_1970_185_069_02.
Guarneros-Meza, V. (2016), EU Foreign Policy towards Latin America, HeinOnline, New York, U.S.A. https://doi.org/10.1057/9781137321282.
Hamidian, M., Shariati, M., Arabnejad, M. and Sinaei, H. (2011), "Assessment of high strength and light weight aggregate concrete properties using ultrasonic pulse velocity technique", *Int. J. Phys. Sci*., **6**(22), 5261-5266. https://doi.org/10.5897/IJPS11.1081.
Heinze, E. (1949), "Besonderer berÜcksichti-dung ihrer verwendung im kältema schinenbau", Kältetechnik, **1**, 26-32.
Heydari, A. and Shariati, M. (2018), "Buckling analysis of tapered BDFGM nano-beam under variable axial compression resting on elastic medium", *Struct. Eng. Mech*., **66**(6), 737-748. https://doi.org/10.12989/sem.2018.66.6.737.
Hosseinpour, E., Baharom, S., Badaruzzaman, W.H.W., Shariati, M. and Jalali, A. (2018), "Direct shear behavior of concrete filled hollow steel tube shear connector for slim-floor steel beams", *Steel Compos. Struct*., **26**(4), 485-499. https://doi.org/10.12989/scs.2018.26.4.485.
Hu, P., Cao, L., Su, J., Li, Q. and Li, Y. (2020), "Distribution characteristics of salt-out particles in steam turbine stage", *Energy*, **192**, 116626. https://doi.org/10.1016/j.energy.2019.116626.
Huang, X., Zhu, Y., Vafaei, P., Moradi, Z. and Davoudi, M. (2021), "An iterative simulation algorithm for large oscillation of the applicable 2D-electrical system on a complex nonlinear substrate", *Eng Comput.*, 1-13. https://doi.org/10.1007/s00366-021-01320-y.
Jahandari, S., Tao, Z., Saberian, M., Shariati, M., Li, J., Abolhasani, M., Kazemi, M., Rahmani, A. and Rashidi, M. (2021), "Geotechnical properties of lime-geogrid improved clayey subgrade under various moisture conditions", *Road Mater. Pavement Des*., 1-19. https://doi.org/10.1080/14680629.2021.1950816.
Jana, T., Mitra, A. and Sahoo, P. (2017), "Dynamic contact interactions of fractal surfaces", *Appl. Surf. Sci*., **392**, 872-882. https://doi.org/10.1016/j.apsusc.2016.09.025.
Jiang, T., Liu, Z., Wang, G. and Chen, Z. (2021a), "Comparative study of thermally stratified tank using different heat transfer materials for concentrated solar power plant", *Energy Reports*, **7**, 3678-3687. https://doi.org/10.1016/j.egyr.2021.06.021.
Jiang, X.P., Wang, Z.T., Zhu, H. and Wang, W.S. (2021b), "Hydraulic turbine system identification and predictive control based on GASA-BPNN", *Int. J. Miner. Metall. Mater*., **28**(7), 1240-1247. https://doi.org/10.1007/s12613-021-2290-6.
Jiao, J., Ghoreishi, S.M., Moradi, Z. and Oslub, K. (2021), "Coupled particle swarm optimization method with genetic algorithm for the static–dynamic performance of the magneto-electro-elastic nanosystem", *Eng Comput*., 1-15. https://doi.org/10.1007/s00366-021-01391-x.
Jin-Shyr, Y. and Nanming, C. (1989), "Short term hydrothermal coordination using multi-pass dynamic programming", *IEEE T. Power Syst*., **4**(3), 1050-1056. https://doi.org/10.1109/59.32598.
Katebi, J., Shoaei-parchin, M., Shariati, M., Trung, N.T. and Khorami, M. (2019), "Developed comparative analysis of metaheuristic optimization algorithms for optimal active control of structures", *Eng Comput*., 1-20. https://doi.org/10.1007/s00366-019-00780-7.
Kearton, W. and Keh, T. (1952), "Leakage of air through labyrinth glands of staggered type", *Proceedings of the Institution of Mechanical Engineers*, **166**(1), 180-195. https://doi.org/10.1243/PIME_PROC_1952_166_022_02.
Khorami, M., Alvansazyazdi, M., Shariati, M., Zandi, Y., Jalali, A. and Tahir, M. (2017a), "Seismic performance evaluation of buckling restrained braced frames (BRBF) using incremental nonlinear dynamic analysis method (IDA)", *Earthq. Struct*., **13**(6), 1-8. http://doi.org/10.12989/eas.2017.13.6.531.
Khorami, M., Khorami, M., Motahar, H., Alvansazyazdi, M., Shariati, M., Jalali, A. and Tahir, M.M. (2017b), "Evaluation of the seismic performance of special moment frames using incremental nonlinear dynamic analysis", *Struct. Eng. Mech*., **63**(2), 259-268. https://doi.org/10.12989/sem.2017.63.2.259.
Khorramian, K., Maleki, S., Shariati, M., Jalali, A. and Tahir, M. (2017), "Numerical analysis of tilted angle shear connectors in steel-concrete composite systems", *Steel Compos. Struct*., **23**(1), 67-85. https://doi.org/10.12989/scs.2017.23.1.067.
Khorramian, K., Maleki, S., Shariati, M. and Ramli Sulong, N.H. (2016), "Behavior of tilted angle shear connectors", *PLoS One*, **10**(12), e0144288. https://doi.org/10.1371/journal.pone.0144288.
Ko, S. and Rhode, D. (1992), "Thermal details in a rotor–stator cavity at engine conditions with a mainstream", *J. Turbomach*., **114**(2), 446-453. https://doi.org/10.1115/1.2929164.
Lattime, S. and Steinetz, B. (2002), "Turbine engine clearance control systems: current practices and future directions", *Proceedings of the 38th AIAA/ASME/SAE/ASEE Joint Propulsion Conference & Exhibit*, Ohio, U.S.A., July. https://doi.org/10.2514/6.2002-3790.
Li, D., Toghroli, A., Shariati, M., Sajedi, F., Bui, D.T., Kianmehr, P., Mohamad, E.T. and Khorami, M. (2019), "Application of polymer, silica-fume and crushed rubber in the production of Pervious concrete", *Smart. Struct. Syst*., **23**(2), 207-214. https://doi.org/10.12989/sss.2019.23.2.207.
Li, Y., Wang, S., Xu, T., Li, J., Zhang, Y., Xu, T. and Yang, J. (2021), "Novel designs for the reliability and safety of supercritical water oxidation process for sludge treatment", *Process Saf. Environ.*, **149**, 385-398. https://doi.org/10.1016/j.psep.2020.10.049.
Lohrengel, M., Rataj, K. and Münninghoff, T. (2016), "Electrochemical machining-mechanisms of anodic dissolution", *Electrochimica Acta*, **201**, 348-353. https://doi.org/10.1016/j.electacta.2015.12.219.
Lucas, G. (1990), "Thermo-mechanical design of the Dresser–Rand EA-418 low pressure CAES expander secondary flow system", Paper No. C403/036, *I Mech. E. Conference*, Brussels, Belgium.
Luo, Z., Sinaei, H., Ibrahim, Z., Shariati, M., Jumaat, Z., Wakil, K., Pham, B.T., Mohamad, E.T. and Khorami, M. (2019), "Computational and experimental analysis of beam to column joints reinforced with CFRP plates", *Steel Compos. Struct*., **30**(3), 271-280. http://doi.org/10.12989/scs.2019.30.3.271.
Ma, L., Liu, X. and Moradi, Z. (2021), "On the chaotic behavior of graphene-reinforced annular systems under harmonic

excitation", *Eng Comput*., 1-25. https://doi.org/10.1007/s00366-020-01210-9.

Mansouri, I., Shariati, M., Safa, M., Ibrahim, Z., Tahir, M. and Petković, D. (2019), "Analysis of influential factors for predicting the shear strength of a V-shaped angle shear connector in composite beams using an adaptive neuro-fuzzy technique", *J. Intell. Manuf*., **30**(3), 1247-1257. https://doi.org/10.1007/s10845-017-1306-6.

Martin, H. (1908), "Labyrinth packings", *Engineering*, **85**, 35.

Mehrabi, P., Shariati, M., Kabirifar, K., Jarrah, M., Rasekh, H., Trung, N.T., Shariati, A. and Jahandari, S. (2021), "Effect of pumice powder and nano-clay on the strength and permeability of fiber-reinforced pervious concrete incorporating recycled concrete aggregate", *Constr. Build. Mater*., **287**, 122652. https://doi.org/10.1016/j.conbuildmat.2021.122652.

Milovancevic, M., Marinović, J.S., Nikolić, J., Kitić, A., Shariati, M., Trung, N.T., Wakil, K. and Khorami, M. (2019), "UML diagrams for dynamical monitoring of rail vehicles", *Physica A*, 121169. https://doi.org/10.1016/j.physa.2019.121169.

Mohammadhassani, M., Nezamabadi-Pour, H., Suhatril, M. and Shariati, M. (2013), "Identification of a suitable ANN architecture in predicting strain in tie section of concrete deep beams", *Struct. Eng. Mech*., **46**(6), 853-868. https://doi.org/10.12989/sem.2013.46.6.853.

Mohammadhassani, M., Akib, S., Shariati, M., Suhatril, M. and Arabnejad Khanouki, M.M. (2014a), "An experimental study on the failure modes of high strength concrete beams with particular references to variation of the tensile reinforcement ratio", *Eng. Fail. Anal*., **41**, 73-80. https://doi.org/10.1016/j.engfailanal.2013.08.014.

Mohammadhassani, M., Nezamabadi-Pour, H., Suhatril, M. and Shariati, M. (2014b), "An evolutionary fuzzy modelling approach and comparison of different methods for shear strength prediction of high-strength concrete beams without stirrups", *Smart. Struct. Syst*., **14**(5), 785-809. http://doi.org/10.12989/sss.2014.14.5.785.

Mohammadhassani, M., Suhatril, M., Shariati, M. and Ghanbari, F. (2014c), "Ductility and strength assessment of HSC beams with varying of tensile reinforcement ratios", *Struct. Eng. Mech*., **48**(6), 833-848. https://doi.org/10.12989/sem.2013.48.6.833.

Moore, A. (1975), "Gas turbine engine internal air systems: a review of the requirements and the problems", *Am. Soc. Mech. Eng*., **80005**, V001T01A001. https://doi.org/10.1115/75-WA/GT-1.

Munson, J., Grant, D. and Agrawal, G. (2002), "Foil face seal proof-of-concept demonstration testing(for gas turbine engines)", *Proceedings of the 38th AIAA/ASME/SAE/ASEE Joint Propulsion Conference and Exhibit*, Indianapolis, U.S.A.

Naghipour, M., Niak, K.M., Shariati, M. and Toghroli, A. (2020a), "Effect of progressive shear punch of a foundation on a reinforced concrete building behavior", *Steel Compos. Struct*., **35**(2), 279-294. https://doi.org/10.12989/scs.2020.35.2.279.

Naghipour, M., Yousofizinsaz, G. and Shariati, M. (2020b), "Experimental study on axial compressive behavior of welded built-up CFT stub columns made by cold-formed sections with different welding lines", *Steel Compos. Struct*., **34**(3), 347-359. https://doi.org/10.12989/scs.2020.34.3.347.

Nasrollahi, S., Maleki, S., Shariati, M., Marto, A. and Khorami, M. (2018), "Investigation of pipe shear connectors using push out test", *Steel Compos. Struct*., **27**(5), 537-543. http://doi.org/10.12989/scs.2018.27.5.537.

Ni, T., Liu, D., Xu, Q., Huang, Z., Liang, H. and Yan, A. (2020), "Architecture of cobweb-based redundant TSV for clustered faults", *IEEE T VLSI Syst*., **28**(7), 1736-1739. http://doi.org/10.1109/TVLSI.2020.2995094.

Nosrati, A., Zandi, Y., Shariati, M., Khademi, K., Darvishnezhad Aliabad, M., Marto, A., Mu'azu, M., Ghanbari, E., Mandizadeh, M.B. and Shariati, A. (2018), "Portland cement structure and its major oxides and fineness", *Smart. Struct. Syst*., **22**(4), 425-432. https://doi.org/10.12989/sss.2018.22.4.425.

Nouri, K., Sulong, N.R., Ibrahim, Z. and Shariati, M. (2021), "Behaviour of novel stiffened angle shear connectors at ambient and elevated temperatures", *Adv. Steel Constr*., **17**(1), 28-38. https://doi.org/10.18057/IJASC.2021.17.1.4.

Owen, J. and Phadke, U. (1980), "An investigation of ingress for a simple shrouded rotating disc system with a radial outflow of coolant", *Am. Soc. Mech. Eng*., **79658**, V01AT01A049. https://doi.org/10.1115/80-GT-49.

Paknahad, M., Shariati, M., Sedghi, Y., Bazzaz, M. and Khorami, M. (2018), "Shear capacity equation for channel shear connectors in steel-concrete composite beams", *Steel Compos. Struct*., **28**(4), 483-494. https://doi.org/10.12989/scs.2018.28.4.483.

Partovi, F. and Fanaie, N. (2020), "Controlling deflection of long steel I-shaped girder bridge using two V-shaped pre-tensioning cables", *J. Cent. South Univ*., **27**(2), 566-577, https://doi.org/10.1007/s11771-020-4317-y.

Phadke, U. (1985), "Flow visualization in a simple rotor-stator system with throughflow", *Flow Visualization III*, 728-732.

Phadke, U. and Owen, J. (1983), "An investigation of ingress for an "air-cooled" shrouded rotating disk system with radial-clearance seals", *J. Eng. Power*., **105**(1), 178-182. https://doi.org/10.1115/1.3227382.

Phadke, U. and Owen, J. (1988), "Aerodynamic aspects of the sealing of gas-turbine rotor-stator systems: Part 1: The behavior of simple shrouded rotating-disk systems in a quiescent environment", *Int. J. Heat Fluid Fl.*, **9**(2), 98-105. https://doi.org/10.1016/0142-727X(88)90060-4.

Qi, C., Fourie, A., Chen, Q. and Liu, P. (2019), "Application of first-principles theory in ferrite phases of cemented paste backfill", *Miner. Eng*., **133**, 47-51. https://doi.org/10.1016/j.mineng.2019.01.011.

Qi, C., Spagnoli, D. and Fourie, A. (2020), "DFT-D study of single water adsorption on low-index surfaces of calcium silicate phases in cement", *Appl. Surface Sci*., **518**, 146255. https://doi.org/10.1016/j.apsusc.2020.146255.

Razavian, L., Naghipour, M., Shariati, M. and Safa, M. (2020), "Experimental study of the behavior of composite timber columns confined with hollow rectangular steel sections under compression", *Struct. Eng. Mech*., **74**(1), 145-156. https://doi.org/10.12989/sem.2020.74.1.145.

Rezaeian, A., Jahanbakhti, E. and Fanaie, N. (2020), "Numerical study of panel zone in a moment connection without continuity plates", *J. Earthq. Eng*., 1-19. https://doi.org/10.1080/13632469.2019.1695021.

Sadeghipour Chahnasir, E., Zandi, Y., Shariati, M., Dehghani, E., Toghroli, A., Mohamed, E.T., Shariati, A., Safa, M., Wakil, K. and Khorami, M. (2018), "Application of support vector machine with firefly algorithm for investigation of the factors affecting the shear strength of angle shear connectors", *Smart. Struct. Syst*., **22**(4), 413-424. http://doi.org/10.12989/sss.2018.22.4.413.

Safa, M., Sari, P.A., Shariati, M., Suhatril, M., Trung, N.T., Wakil, K. and Khorami, M. (2020), "Development of neuro-fuzzy and neuro-bee predictive models for prediction of the safety factor of eco-protection slopes", *Physica A*, 124046. https://doi.org/10.1016/j.physa.2019.124046.

Safa, M., Shariati, M., Ibrahim, Z., Toghroli, A., Baharom, S.B., Nor, N.M. and Petkovic, D. (2016), "Potential of adaptive neuro fuzzy inference system for evaluating the factors affecting steel-concrete composite beam's shear strength", *Steel Compos. Struct*., **21**(3), 679-688. https://doi.org/10.12989/scs.2016.21.3.679.

Sajedi, F. and Shariati, M. (2019), "Behavior study of NC and HSC RCCs confined by GRP casing and CFRP wrapping", *Steel Compos. Struct.*, **30**(5), 417-432. https://doi.org/10.12989/scs.2019.30.5.417.

Sathiyamoorthy, V., Sekar, T. and Elango, N. (2015), "Optimization of processing parameters in ECM of die tool steel using nanofluid by multiobjective genetic algorithm", *Scientific World J*. https://doi.org/10.1155/2015/895696.

Schramm, V., Willenborg, K., Kim, S. and Wittig, S. (2002), "Influence of a honeycomb facing on the flow through a stepped labyrinth seal", *J. Eng. Gas Turb. Power*, **124**(1), 140-146. https://doi.org/10.1115/1.1403460.

Schubert, N., Schneider, M., Michaelis, A., Manko, M. and Lohrengel, M. (2018), "Electrochemical machining of tungsten carbide", *J. Solid State Electrochem.*, **22**(3), 859-868. https://doi.org/10.1007/s10008-017-3823-9.

Sedghi, Y., Zandi, Y., Shariati, M., Ahmadi, E., Moghimi Azar, V., Toghroli, A., Safa, M., Tonnizam Mohamad, E., Khorami, M. and Wakil, K. (2018), "Application of ANFIS technique on performance of C and L shaped angle shear connectors", *Smart. Struct. Syst.*, **22**(3), 335-340. https://doi.org/10.12989/sss.2018.22.3.335.

Shah, S., Ramli Sulong, N.H., Shariati, M., Khan, R. and Jumaat, M. (2016a), "Behavior of steel pallet rack beam-to-column connections at elevated temperatures", *Thin Wall. Struct.*, **106**, 471-483. https://doi.org/10.1016/j.tws.2016.05.021.

Shah, S., Sulong, N.R., Jumaat, M. and Shariati, M. (2016b), "State-of-the-art review on the design and performance of steel pallet rack connections", *Eng. Fail. Anal.*, **66**, 240-258. https://doi.org/10.1016/j.engfailanal.2016.04.017.

Shah, S., Sulong, N.R., Khan, R., Jumaat, M. and Shariati, M. (2016c), "Behavior of industrial steel rack connections", *Mech. Syst. Signal Pr.*, **70**, 725-740. https://doi.org/10.1016/j.ymssp.2015.08.026.

Shah, S., Sulong, N.R., Shariati, M. and Jumaat, M. (2015), "Steel rack connections: identification of most influential factors and a comparison of stiffness design methods", *PloS One*, **10**(10), e0139422. https://doi.org/10.1371/journal.pone.0139422.

Shahabi, S., Ramli Sulong, N.H., Shariati, M., Mohammadhassani, M. and Shah, S. (2016a), "Numerical analysis of channel connectors under fire and a comparison of performance with different types of shear connectors subjected to fire", *Steel Compos. Struct.*, **20**(3), 651-669. https://10.12989/scs.2016.20.3.651.

Shahabi, S., Ramli Sulong, N.H., Shariati, M. and Shah, S. (2016b), "Performance of shear connectors at elevated temperatures-A review", *Steel Compos. Struct.*, **20**(1), 185-203. https://doi.org/10.12989/scs.2016.20.1.185.

Shariat, M., Shariati, M., Madadi, A. and Wakil, K. (2018), "Computational Lagrangian Multiplier Method by using for optimization and sensitivity analysis of rectangular reinforced concrete beams", *Steel Compos. Struct.*, **29**(2), 243-256. https://doi.org/10.12989/scs.2018.29.2.243.

Shariati, M. (2008), "Assessment of building using none-destructive test techniques (ultra sonic pulse velocity and schmidt rebound hHammer)", Ph.D. Dissertation, Universiti Putra Malaysia, Selangor, Malaysia.

Shariati, M., Ramli Sulong, N.H. and Arabnejad Khanouki, M.M. (2010), "Experimental and analytical study on channel shear connectors in light weight aggregate concrete", *Proceedings of the 4th International Conference on Steel & Composite Structures*, Sydney, Australia, July. https://doi.org/10.3850/978-981-08-6218-3_CC-Fr031.

Shariati, M., Ramli Sulong, N.H., Arabnejad Khanouki, M.M. and Mahoutian, M. (2011a), "Shear resistance of channel shear connectors in plain, reinforced and lightweight concrete", *Sci. Res. Essays*, **6**(4), 977-983, https://doi.org/10.5897/SRE10.1120.

Shariati, M., Ramli Sulong, N.H., Arabnejad Khanouki, M.M., Shafigh, P. and Sinaei, H. (2011b), "Assessing the strength of reinforced concrete structures through Ultrasonic Pulse Velocity and Schmidt Rebound Hammer tests", *Sci. Res. Essays*, **6**(1), 213-220, https://doi.org/10.5897/SRE10.879.

Shariati, M., Ramli Sulong, N.H., Sinaei, H., Arabnejad Khanouki, M.M. and Shafigh, P. (2011c), "Behavior of channel shear connectors in normal and light weight aggregate concrete (experimental and analytical study)", *Adv. Mater. Res.*, **168**, 2303-2307. https://doi.org/10.4028/www.scientific.net/AMR.168-170.2303.

Shariati, A., Ramli Sulong, N.H., Suhatril, M. and Shariati, M. (2012a), "Investigation of channel shear connectors for composite concrete and steel T-beam", *Int. J. Phys. Sci.*, **7**(11), 1828-1831. https://doi.org/10.5897/IJPS11.1604.

Shariati, A., Ramli Sulong, N.H., Suhatril, M. and Shariati, M. (2012b), "Various types of shear connectors in composite structures: A review", *Int. J. Phys. Sci.*, **7**(22), 2876-2890. https://doi.org/10.5897/IJPSx11.004.

Shariati, M., Ramli Sulong, N.H. and Arabnejad Khanouki, M.M. (2012c), "Experimental assessment of channel shear connectors under monotonic and fully reversed cyclic loading in high strength concrete", *Mater. Design*, **34**, 325-331. https://doi.org/10.1016/j.matdes.2011.08.008.

Shariati, M., Ramli Sulong, N.H., Suhatril, M., Shariati, A., Arabnejad Khanouki, M.M. and Sinaei, H. (2012d), "Behaviour of C-shaped angle shear connectors under monotonic and fully reversed cyclic loading: An experimental study", *Mater. Design*, **41**, 67-73. https://doi.org/10.1016/j.matdes.2012.04.039.

Shariati, M., Ramli Sulong, N.H., Suhatril, M., Shariati, A., Arabnejad Khanouki, M.M. and Sinaei, H. (2012e), "Fatigue energy dissipation and failure analysis of channel shear connector embedded in the lightweight aggregate concrete in composite bridge girders", *Proceeding of the 5th International Conference on Engineering Failure Analysis*, Hague, Netherlands, July. http://doi.org/10.1016/j.engfailanal.2014.02.017.

Shariati, M. (2013), "Behaviour of C-shaped shear connectors in stell concrete composite beams", Ph.D. Dissertation, Universiti Malaya, Kuala Lumpur, Malaysia. https://doi.org/10.1061/9780784479735.047.

Shariati, M., Ramli Sulong, N.H., Suhatril, M., Shariati, A., Arabnejad Khanouki, M.M. and Sinaei, H. (2013), "Comparison of behaviour between channel and angle shear connectors under monotonic and fully reversed cyclic loading", *Constr. Build. Mater.*, **38**, 582-593. https://doi.org/10.1016/j.conbuildmat.2012.07.050.

Shariati, A., Shariati, M., Ramli Sulong, N.H., Suhatril, M., Arabnejad Khanouki, M.M. and Mahoutian, M. (2014a), "Experimental assessment of angle shear connectors under monotonic and fully reversed cyclic loading in high strength concrete", *Constr. Build. Mater.*, **52**, 276-283. http://doi.org/10.1016/j.conbuildmat.2013.11.036.

Shariati, M., Shariati, A., Ramli Sulong, N.H., Suhatril, M. and Arabnejad Khanouki, M.M. (2014b), "Fatigue energy dissipation and failure analysis of angle shear connectors embedded in high strength concrete", *Eng. Fail. Anal.*, **41**, 124-134. https://doi.org/10.1016/j.engfailanal.2014.02.017.

Shariati, M., Ramli Sulong, N.H., Shariati, A. and Arabnejad Khanouki, M.M. (2015), "Behavior of V-shaped angle shear connectors: experimental and parametric study", *Mater. Struct.*, **49**(9), 3909-3926. https://doi.org/10.1617/s11527-015-0762-8.

Shariati, M., Ramli Sulong, N.H., Shariati, A. and Kueh, A.B.H. (2016), "Comparative performance of channel and angle shear connectors in high strength concrete composites: An experimental study", *Constr. Build. Mater.*, **120**, 382-392.

https://doi.org/10.1016/j.conbuildmat.2016.05.102.

Shariati, M., Toghroli, A., Jalali, A. and Ibrahim, Z. (2017), "Assessment of stiffened angle shear connector under monotonic and fully reversed cyclic loading", *Proceedings of the 5th International Conference on Advances in Civil, Structural and Mechanical Engineering-CSM*. https://doi.org/10.15224/978-1-63248-132-0-44.

Shariati, M., Tahir, M.M., Wee, T.C., Shah, S., Jalali, A., Abdullahi, M.A.M. and Khorami, M. (2018), "Experimental investigations on monotonic and cyclic behavior of steel pallet rack connections", *Eng. Fail. Anal.*, **85**, 149-166. https://doi.org/10.1016/j.engfailanal.2017.08.014.

Shariati, M., Azar, S.M., Arjomand, M.A., Tehrani, H.S., Daei, M. and Safa, M. (2019a), "Comparison of dynamic behavior of shallow foundations based on pile and geosynthetic materials in fine-grained clayey soils", *Geomech. Eng.*, **19**(6), 473-484. https://doi.org/10.12989/gae.2019.19.6.473.

Shariati, M., Faegh, S.S., Mehrabi, P., Bahavarnia, S., Zandi, Y., Masoom, D.R., Toghroli, A., Trung, N.T. and Salih, M.N. (2019b), "Numerical study on the structural performance of corrugated low yield point steel plate shear walls with circular openings", *Steel Compos. Struct.*, **33**(4), 569-581. https://doi.org/10.12989/scs.2019.33.4.569.

Shariati, M., Mafipour, M.S., Mehrabi, P., Bahadori, A., Zandi, Y., Salih, M.N., Nguyen, H., Dou, J., Song, X. and Poi-Ngian, S. (2019c), "Application of a hybrid artificial neural network-particle swarm optimization (ANN-PSO) model in behavior prediction of channel shear connectors embedded in normal and high-strength concrete", *Appl. Sci.*, **9**(24), 5534. https://doi.org/10.3390/app9245534.

Shariati, M., Mafipour, M.S., Mehrabi, P., Zandi, Y., Dehghani, D., Bahadori, A., Shariati, A., Trung, N.T., Salih, M.N. and Poi-Ngian, S. (2019d), "Application of Extreme Learning Machine (ELM) and Genetic Programming (GP) to design steel-concrete composite floor systems at elevated temperatures", *Steel Compos. Struct.*, **33**(3), 319-332. https://doi.org/10.12989/scs.2019.33.3.319.

Shariati, M., Trung, N.T., Wakil, K., Mehrabi, P., Safa, M. and Khorami, M. (2019e), "Moment-rotation estimation of steel rack connection using extreme learning machine", *Steel Compos. Struct.*, **31**(5), 427-435. https://doi.org/10.12989/scs.2019.31.5.427.

Shariati, M. (2020), "Evaluation of seismic performance factors for tension-only braced frames", *Steel Compos. Struct.*, **35**(4), 599-609. https://doi.org/10.12989/scs.2020.35.4.599.

Shariati, M., Azar, S.M., Arjomand, M.A., Tehrani, H.S., Daei, M. and Safa, M. (2020a), "Evaluating the impacts of using piles and geosynthetics in reducing the settlement of fine-grained soils under static load", *Geomech. Eng.*, **20**(2), 87-101. https://doi.org/10.12989/gae.2020.20.2.087.

Shariati, M., Ghorbani, M., Naghipour, M., Alinejad, N. and Toghroli, A. (2020b), "The effect of RBS connection on energy absorption in tall buildings with braced tube frame system", *Steel Compos. Struct.*, **34**(3), 393-407. https://doi.org/10.12989/scs.2020.34.3.393.

Shariati, M., Grayeli, M., Shariati, A. and Naghipour, M. (2020c), "Performance of composite frame consisting of steel beams and concrete filled tubes under fire loading", *Steel Compos. Struct.*, **36**(5), 587-602. https://doi.org/10.12989/scs.2020.36.5.587.

Shariati, M., Mafipour, M.S., Ghahremani, B., Azarhomayun, F., Ahmadi, M., Trung, N.T. and Shariati, A. (2020d), "A novel hybrid extreme learning machine–grey wolf optimizer (ELM-GWO) model to predict compressive strength of concrete with partial replacements for cement", *Eng. Comput.*, 1-23. https://doi.org/10.1007/s00366-020-01081-0.

Shariati, M., Mafipour, M.S., Haido, J.H., Yousif, S.T., Toghroli, A., Trung, N.T. and Shariati, A. (2020e), "Identification of the most influencing parameters on the properties of corroded concrete beams using an Adaptive Neuro-Fuzzy Inference System (ANFIS)", *Steel Compos. Struct.*, **34**(1), 155-170. https://doi.org/10.12989/scs.2020.34.1.155.

Shariati, M., Mafipour, M.S., Mehrabi, P., Ahmadi, M., Wakil, K., Trung, N.T. and Toghroli, A. (2020f), "Prediction of concrete strength in presence of furnace slag and fly ash using Hybrid ANN-GA (Artificial Neural Network-Genetic Algorithm)", *Smart. Struct. Syst.*, **25**(2), 183-195. https://doi.org/10.12989/sss.2020.25.2.183.

Shariati, M., Shariati, A., Trung, N.T., Shoaei, P., Ameri, F., Bahrami, N. and Zamanabadi, S.N. (2020g), "Alkali-activated slag (AAS) paste: Correlation between durability and microstructural characteristics", *Constr. Build. Mater.*, 120886. https://doi.org/10.1016/j.conbuildmat.2020.120886.

Shariati, M., Tahmasbi, F., Mehrabi, P., Bahadori, A. and Toghroli, A. (2020h), "Monotonic behavior of C and L shaped angle shear connectors within steel-concrete composite beams: an experimental investigation", *Steel Compos. Struct.*, **35**(2), 237-247. https://doi.org/10.12989/scs.2020.35.2.237.

Shariati, M., Mafipour, M.S., Mehrabi, P., Shariati, A., Toghroli, A., Trung, N.T. and Salih, M.N. (2021), "A novel approach to predict shear strength of tilted angle connectors using artificial intelligence techniques", *Eng. Comput.*, **37**(3), 2089-2109. https://doi.org/10.1007/s00366-019-00930-x.

Shariati, M. and Shariati, A. (2021), "Hybridization of metaheuristic algorithms with adaptive neuro-fuzzy inference System to predict load-slip behavior of angle shear connectors at elevated temperatures", *Compos. Struct.*, 114524. https://doi.org/10.1016/j.compstruct.2021.114524.

Sinaei, H., Jumaat, M.Z. and Shariati, M. (2011), "Numerical investigation on exterior reinforced concrete Beam-Column joint strengthened by composite fiber reinforced polymer (CFRP)", *Int. J. Phys. Sci.*, **6**(28), 6572-6579. https://doi.org/10.5897/IJPS11.1225.

Sinaei, H., Shariati, M., Abna, A.H., Aghaei, M. and Shariati, A. (2012), "Evaluation of reinforced concrete beam behaviour using finite element analysis by ABAQUS", *Sci. Res. Essays*, **7**(21), 2002-2009. https://doi.org/10.5897/SRE11.1393.

Stewart, P. and Brasnett, K. (1978), "The contribution of dynamic x-ray to gas turbine air sealing technology", 7• REACLLE 9220 ERo-cSUeSINEFRNC, 8.

Suhatril, M., Osman, N., Sari, P.A., Shariati, M. and Marto, A. (2019), "Significance of surface eco-protection techniques for cohesive soils slope in Selangor, Malaysia", *Geotech. Geol. Eng.*, **37**(3), 2007-2014. https://doi.org/10.1007/s10706-018-0740-3.

Tahmasbi, F., Maleki, S., Shariati, M., Ramli Sulong, N.H. and Tahir, M.M. (2016), "Shear capacity of C-shaped and L-shaped angle shear connectors", *PLoS One*, **11**(8), e0156989. https://doi.org/10.1371/journal.pone.0156989.

Tang, L., Zhu, Q., Zhao, J. and Fan, Z. (2017), "Research on the cathode design and experiments of electrochemical machining a closed impeller internal flow channel", *Int. J. Adv. Manuf. Technol.*, **88**(9-12), 2517-2525. https://doi.org/10.1007/s00170-016-8976-7.

Todd, R.H., Allen, D.K. and Alting, L. (1994), *Manufacturing Processes Reference Guide*, Industrial Press Inc, Connecticut, U.S.A.

Toghroli, A., Mohammadhassani, M., Suhatril, M., Shariati, M. and Ibrahim, Z. (2014), "Prediction of shear capacity of channel shear connectors using the ANFIS model", *Steel Compos. Struct.*, **17**(5), 623-639. http://doi.org/10.12989/scs.2014.17.5.623.

Toghroli, A., Suhatril, M., Ibrahim, Z., Safa, M., Shariati, M. and Shamshirband, S. (2016), "Potential of soft computing approach for evaluating the factors affecting the capacity of steel–

concrete composite beam", *J. Intell. Manuf.*, 1-9. https://doi.org/10.1007/s10845-016-1217-y.

Toghroli, A., Shariati, M., Sajedi, F., Ibrahim, Z., Koting, S., Mohamad, E.T. and Khorami, M. (2018), "A review on pavement porous concrete using recycled waste materials", *Smart. Struct. Syst.*, **22**(4), 433-440. https://doi.org/10.12989/sss.2018.22.4.433.

Trung, N.T., Shahgoli, A.F., Zandi, Y., Shariati, M., Wakil, K., Safa, M. and Khorami, M. (2019a), "Moment-rotation prediction of precast beam-to-column connections using extreme learning machine", *Struct. Eng. Mech.*, **70**(5), 639-647. https://doi.org/10.12989/sem.2019.70.5.639.

Trung, N.T., Alemi, N., Haido, J.H., Shariati, M., Baradaran, S. and Yousif, S.T. (2019b), "Reduction of cement consumption by producing smart green concretes with natural zeolites", *Smart. Struct. Syst.*, **24**(3), 415-425. https://doi.org/10.12989/sss.2019.24.3.415.

Valenti, M. (2001), "Making the cut", *Mech. Eng.*, **123**(11), 64-67. https://doi.org/10.1038/s41579-021-00519-6.

Wang, R.M., Gao, Z.Y., Wang, W.R., Xue, Y. and Fu, D.Y. (2018), "Dynamic characteristics of the planetary gear train excited by time-varying meshing stiffness in the wind turbine", *Int. J. Miner. Metall. Mater.*, **25**(9), 1104-1112. https://doi.org/10.1007/s12613-018-1661-0.

Wang, J., Zhu, P., He, B., Deng, G., Zhang, C. and Huang, X. (2021), "An adaptive neural sliding mode control with ESO for uncertain nonlinear systems", *Int. J Control. Autom.*, **19**(2), 687-697. https://doi.org/10.1007/s12555-019-0972-x.

Wei, X., Shariati, M., Zandi, Y., Pei, S., Jin, Z., Gharachurlu, S., Abdullahi, M.M., Tahir, M.M. and Khorami, M. (2018), "Distribution of shear force in perforated shear connectors", *Steel Compos. Struct.*, **27**(3), 389-399. http://doi.org/10.12989/scs.2018.27.3.389.

Wittig, S., Do¨rr, L. and Kim, S. (1983), "Scaling effects on leakage losses in labyrinth seals", *J. Eng. Power.*, **105**(2), 305-309. https://doi.org/10.1115/1.3227416.

Xie, Q., Sinaei, H., Shariati, M., Khorami, M., Mohamad, E.T. and Bui, D.T. (2019), "An experimental study on the effect of CFRP on behavior of reinforce concrete beam column connections", *Steel Compos. Struct.*, **30**(5), 433-441. https://doi.org/10.12989/scs.2019.30.5.433.

Yazdani, M., Kabirifar, K., Frimpong, B.E., Shariati, M., Mirmozaffari, M. and Boskabadi, A. (2020), "Improving construction and demolition waste collection service in an urban area using a simheuristic approach: A case study in Sydney, Australia", *J. Clean. Prod.*, **280**, 124138. https://doi.org/10.1016/j.jclepro.2020.124138.

Ye, R., Liu, P., Shi, K. and Yan, B. (2020), "State damping control: A novel simple method of rotor UAV with high performance", *IEEE Access*, **8**, 214346-214357. https://doi.org/10.1109/ACCESS.2020.3040779.

Yuan, C.J., Bakar, A.S.H.A., Roslan, M.N., Cheng, C.W., Rosekhizam, M.N.S.M., Ghani, J.A. and Wahid, Z. (2021), "Electrochemical machining (ECM) and its recent development", *Jurnal Tribologi*, **28**, 20-31. https://jurnaltribologi.mytribos.org/v28/JT-28-20-31.pdf.

Zandi, Y., Shariati, M., Marto, A., Wei, X., Karaca, Z., Dao, D., Toghroli, A., Hashemi, M.H., Sedghi, Y. and Wakil, K. (2018), "Computational investigation of the comparative analysis of cylindrical barns subjected to earthquake", *Steel Compos. Struct.*, **28**(4), 439-447. https://doi.org/10.12989/scs.2018.28.4.439.

Zhang, C. and Wang, H. (2019), "Swing vibration control of suspended structure using active rotary inertia driver system: Parametric analysis and experimental verification", *Appl. Sci.*, **9**(15), 3144. https://doi.org/10.3390/app9153144.

Zhang, Q., Chen, X., Huang, Y. and Chen, Y. (2018), "Fractal modeling of fluidic leakage through metal sealing surfaces", *Aip Adv.*, **8**(4), 045310. https://doi.org/10.1063/1.5023708.

Zhao, Y., Moradi, Z., Davoudi, M. and Zhuang, J. (2021), "Bending and stress responses of the hybrid axisymmetric system via state-space method and 3D-elasticity theory", *Eng. Comput.*, 1-23. https://doi.org/10.1007/s00366-020-01242-1.

Zhou, Z.J., Tan, J., Qu, D.D., Li, H., Yum, Y.J. and Lim, H.W. (2011), "High heat loading performance of actively cooled W/Cu FGM-based components", *Int. J. Miner. Metall. Mater.*, **18**(4), 467. https://doi.org/10.1007/s12613-011-0464-3.

Ziaei-Nia, A., Shariati, M. and Salehabadi, E. (2018), "Dynamic mix design optimization of high-performance concrete", *Steel Compos. Struct.*, **29**(1), 67-75. https://doi.org/10.12989/scs.2018.29.1.067.

CC